MIKAILALSYS
Journal of Multidisciplinary Sciences

e-ISSN : 2987-2286
p-ISSN : 2987-3924

Index: Harvard, Boston, Sydney, Copernicus, Sinta 4, Scilit, Semantic, Google, etc

https://doi.org/10.58578/mikailalsys.v4i3.11559

Synthesis and Characterization of Sio_2 Thin Films Derived from Rice Husk Ash Coated with Cuo: Evaluation of Photocatalytic Activity through Methylene Blue Degradation

Afra Hayyunnisa, Riri Jonuarti, Yenni Darvina, Fadhila Ulfa Jhora
Universitas Negeri Padang, Indonesia
hayyunnisaafra@gmail.com

Article Info:

Submitted:	Revised:	Accepted:	Published:
Jun 14, 2026	Jul 12, 2026	Jul 24, 2026	Jul 29, 2026

Abstract

Water pollution caused by synthetic dye effluents that resist natural degradation has intensified the need for stable and environmentally sustainable photocatalytic materials. This study aimed to synthesize and characterize bilayer SiO_2/CuO thin films using silica extracted from rice husk ash (RHA) and to evaluate their photocatalytic activity for methylene blue (MB) degradation. Silica was extracted from agricultural RHA, activated with 1 M HCl, fabricated into thin films through sol–gel and spin-coating techniques, and thermally annealed at 300 °C. X-ray diffraction analysis confirmed the amorphous structure of silica, indicated by a broad diffraction hump centered at $2\theta \approx 22°$, and the formation of monoclinic CuO crystalline phases in the bilayer films. Cross-sectional scanning electron microscopy showed that the pure SiO_2 film had a smooth morphology and a thickness of 3.507 μm, whereas the bilayer SiO_2/CuO film had a total thickness of 5.444 μm and exhibited a distinct porous upper layer comprising accumulated CuO grains deposited on the smooth SiO_2 base layer. Under UV-A irradiation, MB absorbance at $\lambda = 664$ nm decreased continuously, resulting in a degradation efficiency of 12.13% after 180 min. The degradation process closely followed pseudo-first-order kinetics, with a rate constant of 7.33 $\times 10^{-4}$ min^{-1} and $R^2 = 0.985$. These findings demonstrate that biomass-derived silica from RHA can function as a supporting matrix for anchoring photocatalytically active CuO granular structures. This study contributes to the sustainable utilization of agricultural waste and provides a foundation for the further development of biomass-derived thin-film photocatalysts for synthetic dye degradation.

Keywords: Biomass-Derived Silica; Methylene Blue Degradation; Photocatalysis; Rice Husk Ash; SiO_2/CuO Thin Films

INTRODUCTION

Water pollution caused by industrial wastewater containing synthetic dyes and persistent organic pollutants poses a severe threat to aquatic ecosystems and human health because these contaminants exhibit high chemical stability and resistance to natural degradation. Conventional wastewater treatment methods, including adsorption, coagulation, membrane filtration, and biological treatment, have been widely applied to reduce pollutant concentrations. However, these methods still suffer from several limitations, such as the generation of secondary waste, relatively high operational costs, and, in many cases, the transfer of pollutants from one phase to another without complete mineralization. These limitations have encouraged the development of more sustainable treatment technologies capable of completely degrading organic contaminants. Among the available approaches, Advanced Oxidation Processes (AOPs), particularly photocatalysis, have attracted considerable attention because they generate highly reactive oxygen species (ROS), such as hydroxyl radicals (·OH) and superoxide radicals ($\cdot O_2^-$), which can non-selectively oxidize complex organic molecules into simpler intermediates and ultimately mineralize them into CO_2 and H_2O. Owing to its ability to utilize light energy as the driving force while minimizing secondary pollution, photocatalysis has emerged as a promising, energy-efficient, and environmentally friendly technology for wastewater remediation (Iyyappan et al., 2024; Khader et al., 2024; Lee et al., 2023).

To rigorously benchmark the efficacy of photocatalytic systems, standard model pollutants with high structural stability are required. Methylene Blue (MB) is a cationic thiazine dye commonly employed as a benchmark pollutant in photocatalytic investigations owing to its stable aromatic ring system, high water solubility, and characteristic light absorption peak in the UV–Vis spectrum. Consequently, the quantitative degradation of MB serves as a reliable metric for evaluating the catalytic performance of various semiconductor systems (Muzammal et al., 2024; Naggar et al., 2024). Nevertheless, the overall photocatalytic degradation efficiency remains heavily governed by the intrinsic properties, surface area, and architectural configuration of the chosen semiconductor materials.

In recent years, the paradigm of photocatalyst design has shifted not only toward maximizing pollutant degradation efficiency but also toward integrating renewable, low-cost, and eco-friendly biomaterials. Among agricultural waste streams, rice husk ash (RHA) represents an exceptionally promising biogenic resource, containing up to 87–97 wt% silica (SiO_2) after controlled calcination (Nzereogu et al., 2023). Silica derived from RHA possesses a high specific surface area, excellent chemical and thermal stability, non-toxicity, and high potential as a catalyst support matrix. The presence of a silica support enhances the adsorption capacity for pollutant molecules on the catalyst surface, thereby facilitating subsequent photocatalytic reactions. However, because pure SiO_2 features a wide energy band gap ~8.9 eV, it cannot be photo-activated under solar or near-UV light independently, necessitating its coupling with narrow-band-gap active semiconductors (Rodriguez-Otero et al., 2023).

Copper(II) oxide (CuO) is a p-type semiconductor featuring a direct band gap of 1.2–2.0 eV, which enables efficient photon absorption within the visible and near-UV spectrum. This optical property makes CuO an outstanding candidate for generating photogenerated electron-hole (e^-/h^+) pairs under light illumination (Jonuarti et al., 2026). Nevertheless, utilizing CuO in powder form suffers from severe practical drawbacks, including particle agglomeration, difficulties in post-reaction recovery from aqueous media, and potential mass loss during recycling steps. Immobilizing CuO into thin-film architectures offers a practical strategy to overcome these recovery challenges, enhancing reusability while eliminating secondary particle separation steps (Sarma, 2023).

Coupling SiO_2 and CuO into a bilayer thin-film configuration is anticipated to yield synergistic effects that enhance photocatalytic performance. In this bilayer layout, the underlying SiO_2 layer functions as a smooth, high-surface-area foundation, while the upper CuO layer acts as the photoactive component responsible for absorbing photons and generating reactive radicals (Federico et al., 2025; Huyen et al., 2022). However, the functional efficacy of such bilayer systems is critically dependent on layer thickness, interfacial contact quality, and cross-sectional morphology. Without direct microstructural and thickness characterization across the film cross-section, the precise relationship between physical film architecture and photocatalytic performance cannot be comprehensively resolved.

Although several prior studies have investigated silica-CuO composites in powder or nanoparticle forms, investigations into bilayer SiO_2/CuO thin films utilizing biogenic RHA-derived silica—specifically linking cross-sectional SEM morphology with photocatalytic degradation kinetics—remain scarce. Therefore, this study addresses this research gap by synthesizing bilayer SiO_2/CuO thin films via combined sol-gel and spin-coating processes. The main novelty of this work lies in establishing the direct correlation between crystal phase evolution (XRD), cross-sectional morphological properties including vertical film thickness and granular phase distribution (cross-sectional SEM), and evaluate their photocatalytic activity toward methylene blue degradation using UV–Vis spectroscopy.

METHODS

Raw rice husk collected from a local rice mill in Padang, West Sumatra, Indonesia, served as the biogenic silica precursor. Analytical grade reagents used without further purification included hydrochloric acid (HCl, 37%, Robogen Laboratory Chemicals), sodium hydroxide (NaOH, 98%, Merck), copper(II) oxide powder (CuO, Cifala Laboratorium Centre), polyvinylpyrrolidone (PVP-K30, Unilong Industry), absolute ethanol (99.9%, Merck), and deionized water.

Silica was extracted following the method described by (Dorairaj et al., 2022) with slight modifications. Raw rice husk was thoroughly washed with running water to eliminate adhering dirt, then dried in an oven at 100 °C for 24 h. A 50 g portion of dried rice husk was soaked in 500 mL of 1 M HCl solution and heated at 80 °C under continuous magnetic stirring (200–300 rpm) for 2 h to leach out metallic impurities. After cooling to room temperature, the mixture was filtered and washed with hot deionized water (50–60 °C) until reaching a neutral pH (6–7). The leached husk was dried at 100 °C for 24 h and calcined in a muffle furnace at 650 °C for 4 h (heating rate of 5 °C/min) to obtain high-purity white rice husk ash (RHA) silica (SiO_2).

To further enhance purity and surface porosity, acid activation was performed using 1 M HCl at a solid-to-liquid ratio of 1:10 (w/v). Typically, 1 g of calcined RHA silica powder was suspended in 10 mL of 1 M HCl, stirred, and heated at 80 °C for 2 h. Following activation, the slurry was filtered and rinsed repeatedly with warm deionized water until the filtrate reached pH 7. The activated silica precipitate was dried at 100 °C until reaching constant mass prior to sol preparation (Hidayat et al., 2026).

The silica sol was prepared according to the method adapted from (Rahmadhani et al., 2024). Briefly, 0.3 g of activated silica powder was dissolved in 10 mL of 1 M NaOH solution and heated at 80–90 °C for 1 h to form a sodium silicate (Na_2SiO_3) solution. The solution was subsequently neutralized by slow dropwise addition of 1 M HCl until reaching pH 7–8, forming a silica gel. The gel was aged for 24 h at ambient temperature and washed with deionized water to remove residual NaCl salts. Finally, the cleaned gel was dispersed in a mixture of 6 mL ethanol and 2 mL deionized water, followed by ultrasonication for 30 min to yield a homogeneous, stable SiO_2 sol (Adam et al., 2025).

Glass microscope slides (*1* cm × *1* cm) were ultrasonically cleaned sequentially in acetone, ethanol, and deionized water for 10 min each, then dried under nitrogen gas flow (Bitu et al., 2023). A 150 µL aliquot of SiO_2 sol was deposited onto the glass substrate via a two-stage spin-coating process: 400 rpm for 30 s (spreading stage) followed by 3000 rpm for 30 s (thinning stage). The deposited SiO_2 film was thermally annealed in a furnace at 300 °C for 3 h at a heating rate of 5 °C/min (Walker & Koutsos, 2023). Concurrently, a CuO suspension was prepared by dispersing 0.1 g of CuO powder and 0.05 g of PVP-K30 in 10 mL of absolute ethanol, followed by ultrasonication for 60 min. A 150 µL volume of the CuO suspension was spin-coated onto the pre-annealed SiO_2 film using identical rotational parameters. The resulting bilayer SiO_2/CuO film was post-annealed at 300 °C for 3 h to promote interfacial adhesion and enhance CuO crystallinity (Kekuda, 2024).

The phase composition and crystal structure of the materials were characterized using X-ray diffraction (XRD) on two types of samples: silica powder extracted from rice husk ash before and after the activation process, and the SiO2/CuO thin films. The analysis of silica powder was intended to identify the diffraction characteristics of SiO2 and evaluate the effect of the activation process on the material structure. Meanwhile, the analysis of the SiO2/CuO thin films was conducted to identify the crystalline phase of CuO and confirm the presence of SiO2 based on the obtained diffraction patterns. The diffraction data were subsequently analyzed using Origin and Match software.

Cross-sectional morphology, physical film thickness, and interfacial structure were analyzed using a Scanning Electron Microscope (SEM, JEOL JSM-6360). Samples were fractured precisely along the cross-section and sputter-coated with a thin gold layer to prevent electrostatic charging. SEM imaging was performed at an accelerating voltage of 15 kV and a magnification of 15,000×. Cross-sectional microstructural analysis focused on measuring vertical film thicknesses, assessing surface flatness, and observing the distribution of the upper CuO granular phase.

Photocatalytic activity was evaluated by monitoring the degradation of methylene blue (MB) dye (10 mg/L initial concentration). The bilayer SiO_2/CuO thin film was placed at the bottom of a glass reactor containing 50 mL of MB solution. Before light exposure, the system was kept in the dark for 30 min under mild stirring to establish adsorption-desorption equilibrium between dye molecules and the film surface (Ulfa, 2022). Subsequently, the reactor was irradiated under a UV-A lamp ($\lambda = 365$ nm, 15 W) placed 10 cm above the solution level. At 0, 60, 120, and 180 min of exposure, 3 mL aliquots were extracted, and MB absorbance was measured at its maximum absorption wavelength ($\lambda_{\max} = 664$ nm) using a UV-Vis spectrophotometer (Shimadzu UV-1800). The degradation efficiency (η) was calculated using Equation (1):

$$\eta(\%) = \frac{C_0 - C_t}{C_0} \times 100\% \qquad (1)$$

where C_0 is the initial MB concentration and C_t is the concentration at irradiation time t (Jonuarti et al., 2026).

RESULTS

1. XRD Characterization of Silica Powder Before and After Activation

The X-ray diffraction (XRD) patterns of silica (SiO_2) powder extracted from rice husk ash before and after activation using a 1 M HCl solution are presented in Figure 1(a–b). Figure 1(a) shows the diffraction pattern of the silica powder before activation, whereas Figure 1(b) presents the diffraction pattern after activation. In general, the activation process altered the diffraction characteristics, as indicated by the reduction in the intensity of several crystalline peaks and the appearance of a broad hump at approximately $2\theta \approx 22°$. In addition, the diffraction pattern prior to activation still exhibited several peaks associated with impurity compounds, whereas after activation the pattern was dominated by the characteristic features of amorphous SiO_2. These results indicate that the activation process affected the structural characteristics of the silica powder. A more detailed discussion regarding phase identification and the influence of activation on the silica structure is provided in the Discussion section.

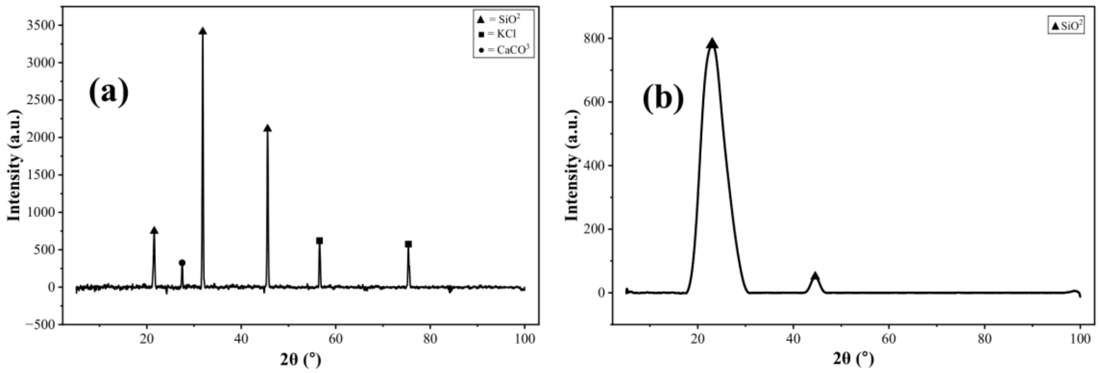

Figure 1. X-ray diffraction (XRD) patterns of silica (SiO_2) powder extracted from rice husk ash: (a) before activation and (b) after activation using a 1 M HCl solution.

Figure 1 shows the X-ray diffraction (XRD) patterns of silica (SiO_2) powder extracted from rice husk ash before and after activation with a 1 M HCl solution. A comparison of the two diffraction patterns reveals changes in peak intensity and diffraction characteristics, indicating the effect of the activation process on the silica structure. HCl activation plays a role in removing impurities and improving the purity of the resulting silica.

2. XRD Characterization of SiO_2 and Bilayer SiO_2/CuO Thin Films

The X-ray diffraction (XRD) patterns of the SiO_2 thin films and bilayer SiO_2/CuO thin films synthesized using the spin-coating method are presented in Figure 2(a–b). Figure 2(a) shows the diffraction pattern of the SiO_2 thin film, while Figure 2(b) displays the diffraction pattern of the bilayer SiO_2/CuO thin film after CuO deposition. The differences in diffraction characteristics between the two samples indicate structural changes following the formation of the bilayer film. A detailed discussion of the crystal phases and structural characteristics of each layer is provided in the Discussion section.

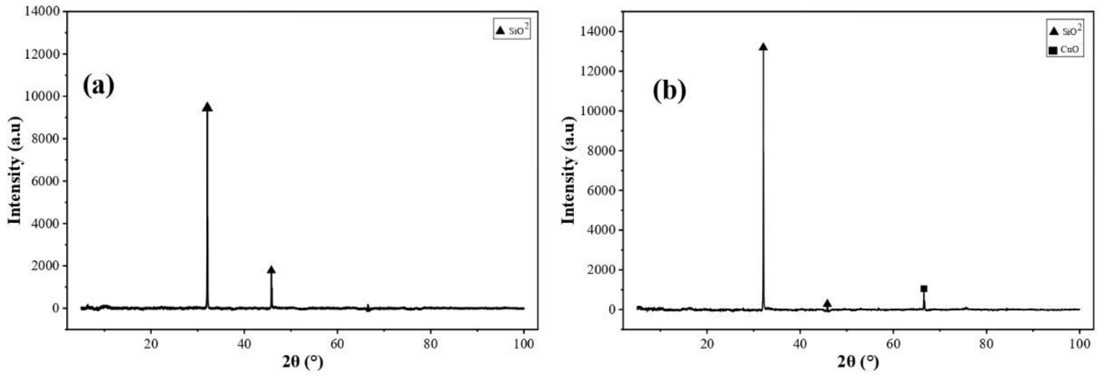

Figure 2. X-ray diffraction (XRD) patterns of thin films deposited on glass substrates : (a) SiO_2 thin film and (b) bilayer SiO_2/CuO thin film.

Figure 2 presents the X-ray diffraction (XRD) patterns of thin films deposited on glass substrates, namely the SiO_2 thin film and the bilayer SiO_2/CuO thin film. A comparison of the diffraction patterns reveals changes in diffraction peak characteristics after the addition of the CuO layer, indicating the formation of a bilayer structure on the substrate surface. These results demonstrate that the deposition process successfully produced thin films with the intended composition.

3. Cross-Sectional SEM Morphological Analysis

High-resolution cross-sectional SEM micrographs (15,000× magnification) for single-layer SiO_2 and bilayer SiO_2/CuO films are shown in Figure 3(a–b). In Figure 3(a), the pure SiO_2 film displays a dense, continuous single-layer structure adhering firmly to the glass substrate, characterized by a smooth upper boundary (*SiO_2 Surface*). Quantitative image analysis revealed a uniform vertical thickness of 3.507 μm for this pure silica base.

Conversely, Figure 3(b) demonstrates that the bilayer SiO_2/CuO film exhibits an increased total thickness of 5.444 μm. Overlying the smooth SiO_2 foundation, a distinct porous secondary layer consisting of clustered particulate grains (*CuO Granular Phase*) is clearly resolved. The net vertical thickness increase of ∼ *1.937* μm corresponds to the effective thickness of the deposited granular CuO top layer.

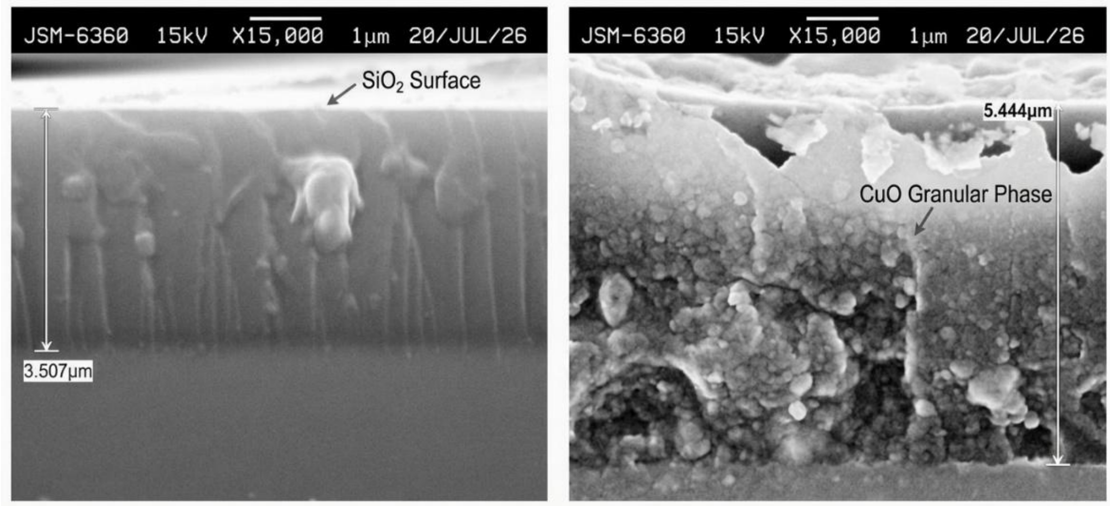

(a) SEM of SiO_2 Thin Film 15,000x (b) SEM of SiO_2/CuO Thin Film 15,000x

Figure 3. SEM Analysis of Thin Films. (a) 15,000× magnification of pure SiO_2 layer (~ *3.5* μm thickness). (b) 15,000× magnification of SiO_2/CuO composite layer (~ *5.4* μm thickness), showing the distributed granular CuO phase.

This cross-sectional architecture—combining a 3.507 μm silica support with a 5.444 μm total bilayer profile—directly influences active site availability during photocatalytic dye degradation.

4. Photocatalytic Activity of SiO_2/CuO Thin Films

To evaluate the photocatalytic activity of the SiO_2/CuO thin films, degradation experiments of methylene blue (MB) solution were conducted using UV–Vis spectroscopy at different irradiation times, namely 0, 60, 120, and 180 min. Changes in the intensity of the MB absorption peak at the maximum wavelength were used to determine the degradation efficiency, the relative concentration ratio (C/C_0), and the reaction kinetics based on the pseudo-first-order model. The experimental results are presented in Figure 3.

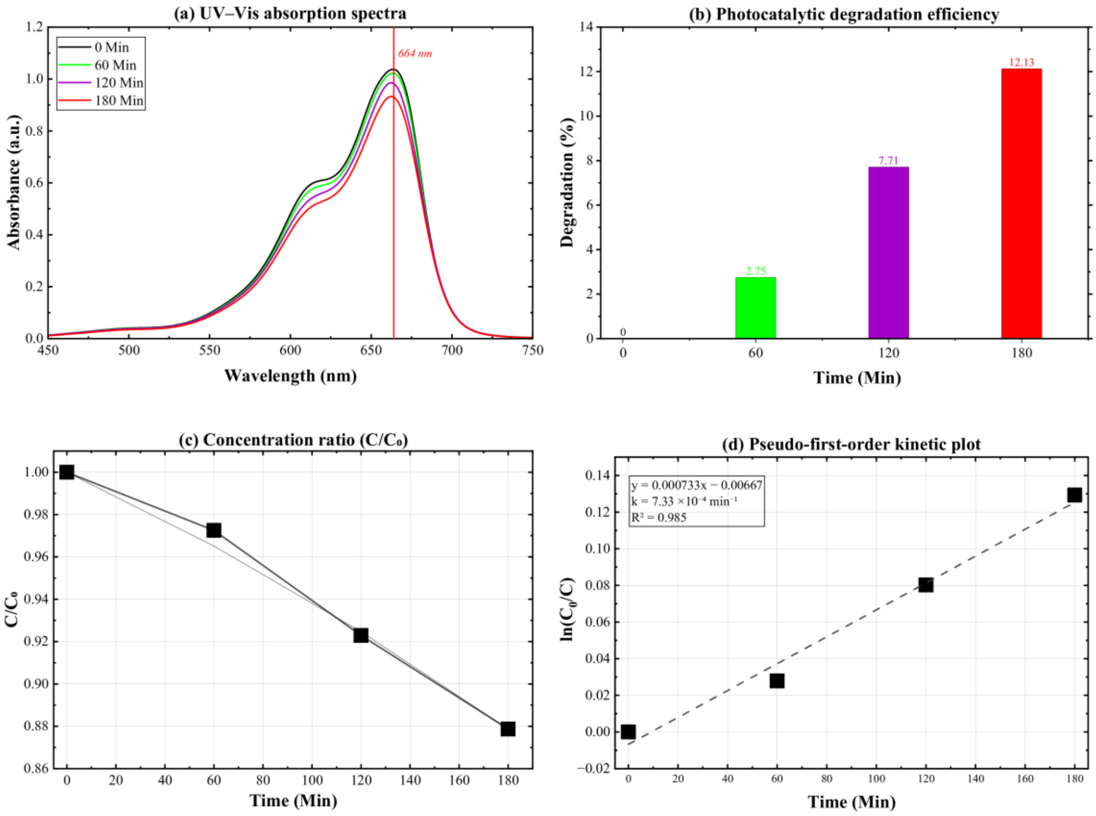

Figure 4. Photocatalytic activity of SiO_2/CuO thin films toward methylene blue (MB) degradation.

Figure 4 illustrates the photocatalytic performance of the SiO_2/CuO thin films in degrading methylene blue (MB): (a) UV–Vis absorbance spectra recorded at irradiation times of 0, 60, 120, and 180 min, with the main absorption peak located at approximately 664 nm; (b) degradation efficiency of MB at each irradiation time; (c) variation in the relative concentration ratio (C/C_0) as a function of irradiation time; and (d) the pseudo-first-order kinetic plot based on the relationship between $\ln(C_0/C)$ and irradiation time, yielding a reaction rate constant (k) of 7.33×10^{-4} min^{-1} and a coefficient of determination (R^2) of 0.985.

DISCUSSION

1. XRD Characterization of Silica Powder Before and After Activation

The X-ray diffraction patterns presented in Figure 1(a) indicate that the silica powder extracted from rice husk ash before activation still exhibited several diffraction peaks with relatively high intensities. These peaks suggest the presence of crystalline impurities originating from elements such as Ca, K, Fe, and Mg, indicating that the diffraction pattern was not solely dominated by the SiO_2 phase.

After activation using a 1 M HCl solution, the diffraction pattern in Figure 1(b) changed significantly, as evidenced by the appearance of a broad hump at approximately $2\theta \approx 22°$, while most of the crystalline peaks decreased in intensity or disappeared. This change indicates that HCl activation effectively removed a large proportion of the impurities without altering the fundamental structure of SiO_2, thereby improving the relative purity of the extracted silica.

The predominance of the amorphous phase provides advantages for photocatalytic applications because it offers a larger surface area, which can enhance methylene blue adsorption and provide more favorable sites for CuO deposition. These findings are consistent with those reported by (Rahmadhani et al., 2024; Rodriguez-otero et al., 2023; Nzereogu et al., 2023), who demonstrated that acid activation produces amorphous silica characterized by a broad hump around 22°.

2. XRD Characterization of SiO_2 and Bilayer SiO_2/CuO Thin Films

The diffraction pattern of the SiO_2 thin film shown in Figure 2(a) is dominated by an amorphous phase with relatively low intensity. This behavior can be attributed to the small film thickness and the use of an amorphous glass substrate, which increases the diffraction background and reduces the visibility of the SiO_2 peaks.

Following CuO deposition via the spin-coating method, the diffraction pattern in Figure 2(b) exhibits several peaks associated with the monoclinic CuO phase. The appearance of these peaks confirms the successful formation of the CuO layer on the SiO_2 surface. However, the CuO diffraction peaks remain relatively weak due to the thin film thickness, small crystallite size, the dominant signal from the glass substrate, and the possible presence of preferred orientation. Furthermore, the annealing temperature of 300 °C is presumed to be insufficient for achieving optimal CuO crystallinity.

These results demonstrate that the bilayer SiO_2/CuO thin films were successfully synthesized. In this structure, SiO_2 acts as the supporting material, while CuO serves as the active component responsible for light absorption during the photocatalytic process. Previous studies have reported that the incorporation of CuO onto a stable SiO_2 support can improve the dispersion of CuO particles, provide a larger active surface area, and enhance the interaction between the photocatalyst and target pollutants during photocatalytic degradation processes (Rodriguez-Otero et al., 2023).

3. Cross-Sectional Morphological Analysis and Interfacial Characteristics

Cross-sectional SEM analysis Figure 3 provides crucial structural insights into the physical layout of the bilayer system. For single-layer SiO_2 Figure 3(a), the 3.507 μm thick film displays excellent continuity and strong substrate adhesion without micro-cracks. This indicates that the two-stage spin coating process (400 rpm/3000 rpm) combined with 300 °C thermal consolidation yields a highly uniform silica base.

For the bilayer film Figure 3(b), the total thickness expansion to 5.444 μm confirms the successful deposition of an upper CuO layer measuring ~1.9 μm in thickness. Unlike the smooth silica base, the top CuO layer exhibits a granular, porous cross-sectional morphology (*CuO Granular Phase*). The formation of this granular texture is assisted by PVP-K30, which acts as a steric stabilizer during suspension synthesis to prevent severe mass agglomeration. This porous granular architecture is beneficial for catalysis, as it increases active surface area and promotes dye penetration into the porous layer.

4. Photocatalytic Activity of Bilayer SiO_2/CuO Thin Films

The photocatalytic activity of the SiO_2/CuO thin films toward the degradation of methylene blue (MB) under irradiation for up to 180 min is presented in Figure 4. The photocatalytic performance was evaluated based on changes in the UV–Vis absorbance spectra, degradation efficiency, the relative concentration ratio (C/C_0), and pseudo-first-order reaction kinetics.

Figure 4(a) shows that the absorbance peak of methylene blue remained at approximately 664 nm, although its intensity gradually decreased with increasing irradiation time. The reduction in absorbance indicates a decrease in methylene blue concentration as a result of the photodegradation process. Under UV irradiation, CuO generates electron–hole pairs that subsequently produce reactive species, such as hydroxyl radicals (•OH) and superoxide radicals ($•O_2^-$), which oxidize methylene blue molecules. The absence of any peak shift suggests that the degradation process is primarily governed by the reduction in dye concentration.

As shown in Figure 4(b), the degradation efficiency increased from 2.75% after 60 min to 7.71% after 120 min and reached 12.13% after 180 min of irradiation. This trend indicates that the photodegradation process proceeded continuously throughout the irradiation period. Nevertheless, the overall degradation efficiency remains relatively low. This limitation is likely due to the limited amount of CuO deposited on the SiO_2 surface, as the spin-coating process was performed using only a single deposition cycle. Consequently, the resulting film was relatively thin, reducing the number of active sites available for interaction with methylene blue molecules.

In addition, the use of conventional glass slides as substrates restricted the annealing temperature to approximately 300 °C in order to prevent substrate deformation or cracking. The relatively low annealing temperature hindered the development of CuO crystallinity, leading to a high recombination rate of electron–hole pairs and reducing the efficiency of hydroxyl radical (•OH) and superoxide radical (•O_2^-) generation. These findings are in agreement with the study reported by (Kekuda, 2024), which demonstrated that increasing the annealing temperature to 400–500 °C significantly enhances CuO crystallinity and improves its photocatalytic performance.

Figure 4(c) illustrates that the C/C_0 value decreased from 1.00 to approximately 0.88 after 180 min of irradiation. This decrease confirms that the methylene blue concentration gradually declined due to photodegradation. The relatively slow degradation rate suggests that further optimization of the film crystallinity, thickness, and porosity is required to improve photocatalytic activity. Figure 4(d) presents the linear relationship between $\ln(C_0/C)$ and irradiation time, yielding the regression equation: y = 0.000733x - 0.00667 with a coefficient of determination (R^2) of 0.985. The corresponding reaction rate constant was calculated to be ($k = 7{,}33 \times 10^{-4}\ \mathrm{min}^{-1}$) . The high R^2 value indicates that methylene blue degradation follows the pseudo-first-order kinetic model. The relatively low value of the rate constant is consistent with the limited degradation efficiency and is likely associated with the small active surface area and the restricted annealing temperature imposed by the use of glass substrates (Samarasekara & Premasiri, 2018).

Overall, the SiO_2/CuO thin films exhibited photocatalytic activity toward methylene blue degradation, although both the degradation efficiency and reaction rate constant remained relatively low. Improved performance may be achieved by employing substrates with higher thermal resistance, thereby enabling annealing at elevated temperatures to enhance CuO crystallinity and photocatalytic activity.

CONCLUSION

Bilayer SiO_2/CuO thin films were successfully synthesized using biogenic silica extracted from rice husk ash via combined sol-gel and spin-coating techniques. XRD analysis confirmed that 1 M HCl activation yielded high-purity amorphous silica ($2\theta \approx 22°$) and that subsequent CuO deposition formed monoclinic CuO crystalline phases. Cross-sectional SEM imaging verified the physical bilayer structure, showing a smooth 3.507 μm thick SiO_2 base film and a 5.444 μm total thickness for the bilayer film featuring a porous *CuO Granular Phase* upper layer. Photocatalytic tests demonstrated that the bilayer SiO_2/CuO film achieved 12.13% MB degradation after 180 min of UV-A irradiation ($C/C_0 = 0.88$). The degradation process strictly obeyed pseudo-first-order reaction kinetics with a rate constant (k) of 7.33×10^{-4} min^{-1} ($R^2 = 0.985$). These results highlight the efficacy of agricultural RHA-derived silica as a functional support for thin-film photocatalysts. Future studies should optimize spin-coating cycle repetitions and employ heat-resistant substrates to allow annealing above 300 °C, thereby maximizing CuO crystallinity and overall photocatalytic efficiency.

This study contributes to the utilization of rice husk ash as an alternative silica source for the development of thin-film photocatalytic materials. In addition to demonstrating the successful fabrication of SiO_2/CuO bilayer thin films through the spin-coating method, this research highlights the potential of extracted silica as a supporting material for CuO in the degradation of organic dyes. These findings provide a foundation for the development of more economical and environmentally friendly photocatalytic materials derived from agricultural waste.

For future research, further optimization of spin-coating cycles, film thickness, and SiO_2/CuO composition is recommended to improve photocatalytic activity. In addition, the use of substrates with higher thermal resistance should be considered to enable annealing at temperatures above 300 °C, resulting in improved CuO crystallinity. Further investigations regarding the effects of different light sources, operational conditions, and other photocatalytic parameters are also required to achieve higher degradation efficiency.

REFERENCES

Adam, J. A., Oboh, I. O., Etuk, V. E., Okon, F. E., & Asangausung, P. E. (2025). Extraction of silica from rice husk for the production and optimization of metallurgical-grade silicon for potential engineering applications. *World Journal of Advanced Research and Reviews, 25*(3), 2413–2433. https://doi.org/10.30574/wjarr.2025.25.3.0961

Bitu, M. N. A., Tanvir, N. I., Islam, S., & Farhad, S. F. U. (2023). Effect of substrate surface on the wide bandgap SnO_2 thin films grown by spin coating. *MRS Advances, 8*, 194–200. https://doi.org/10.1557/s43580-023-00515-3

Dorairaj, D., Govender, N., Zakaria, S., & Wickneswari, R. (2022). Green synthesis and characterization of UKMRC-8 rice husk-derived mesoporous silica nanoparticle for agricultural application. *Scientific Reports, 12*, 20162. https://doi.org/10.1038/s41598-022-24484-z

El-Naggar, M. A., Maghawry, A. H., Alturki, A. A., Nosier, S. A., Hussein, M., & Abdel-Aziz, M. H. (2024). TiO_2-catalyzed photodegradation of methylene blue in a helical FEP tubing reactor: Modeling and optimization using response surface methodology. *Applied Water Science, 14*(9), 207. https://doi.org/10.1007/s13201-024-02205-3

Federico, A., Dhaneswara, D., Sudiro, T., Pradana, A. F., Suhariadi, I., Surip, S. N., & Fatriansyah, J. F. (2025). TiO_2-functionalized mesoporous silica thin films synthesized by spin-coating to enhance methylene blue and methyl orange removal efficiency. *Chemical Physics Impact, 11*, 100897. https://doi.org/10.1016/j.chphi.2025.100897

Iyyappan, J., Gaddala, B., Gnanasekaran, R., Gopinath, M., Yuvaraj, D., & Kumar, V. (2024). Critical review on wastewater treatment using photocatalytic advanced oxidation process: Role of photocatalytic materials, reactor design and kinetics. *Case Studies in Chemical and Environmental Engineering, 9*, 100599. https://doi.org/10.1016/j.cscee.2023.100599

Jagadish, K. A., & Kekuda, D. (2024). Thermal annealing effect on phase evolution, physical properties of DC sputtered copper oxide thin films and transport behavior of ITO/CuO/Al Schottky diodes. *Applied Physics A, 130*, 315. https://doi.org/10.1007/s00339-024-07464-0

Jonuarti, R., Anugrah, M. R., Hidayat, R., Kurniawati, Y., Diño, W. A., & Harumningtyas, A. A. (2026). Engineering core@shell Fe_2O_3@CuO nanocubes toward efficient photocatalysis: Structural design and DFT mechanistic study. *Materials Science and Engineering: B, 332*, 119680. https://doi.org/10.1016/j.mseb.2026.119680

Khader, E. H., Muslim, S. A., Cata Saady, N. M., Ali, N. S., Salih, I. K., Mohammed, T. J., Albayati, T. M., & Zendehboudi, S. (2024). Recent advances in photocatalytic advanced oxidation processes for organic compound degradation: A review. *Desalination and Water Treatment, 318*, 100384. https://doi.org/10.1016/j.dwt.2024.100384

Lee, D. E., Kim, M. K., Danish, M., & Jo, W. K. (2023). State-of-the-art review on photocatalysis for efficient wastewater treatment: Attractive approach in photocatalyst design and parameters affecting the photocatalytic degradation. *Catalysis Communications, 183*, 106764. https://doi.org/10.1016/j.catcom.2023.106764

Muzammal, S., Ahmad, A., Sheraz, M., Kim, J., Ali, S., Hanif, M. B., Hussain, I., Pandiaraj, S., Alodhayb, A., Javed, M. S., Al-Bonsrulah, H. A. Z., & Motola, M. (2024). Polymer-supported nanomaterials for photodegradation: Unraveling the methylene blue menace. *Energy Conversion and Management: X, 22*, 100547. https://doi.org/10.1016/j.ecmx.2024.100547

Nzereogu, P. U., Omah, A. D., Ezema, F. I., Iwuoha, E. I., & Nwanya, A. C. (2023). Silica extraction from rice husk: Comprehensive review and applications. *Hybrid Advances, 4*, 100111. https://doi.org/10.1016/j.hybadv.2023.100111

Pham Ngoc, K. H., & Vu, A.-T. (2022). Simple preparation of the $CuO \cdot Fe_3O_4$/silica composite from rice husk for enhancing Fenton-like catalytic degradation of tartrazine in a wide pH range. *Adsorption Science & Technology, 2022*, 6454354. https://doi.org/10.1155/2022/6454354

Ratnawulan, Rahmadhani, D., Zulkifli, Yuliani, K. D., Frida, E., & Taufiq, A. (2024). Hydrophobic and antibacterial properties of textiles using nanocomposite chitosan and SiO_2 from rice husk ash as-coating. *South African Journal of Chemical Engineering, 48*, 366–374. https://doi.org/10.1016/j.sajce.2024.03.010

Risfaheri, Hidayat, T., Yuliani, S., Hoerudin, Wahyuningsih, K., Yulianto, A., Setyawan, N., Winarti, C., & Arif, A. B. (2026). Sustainable production of high-purity amorphous silica from rice husk: A comparative study on the impact of fresh and reused hydrochloric acid leaching. *South African Journal of Chemical Engineering, 56*, 100848. https://doi.org/10.1016/j.sajce.2026.100848

Rodriguez-Otero, A., Vargas, V., Galarneau, A., Castillo, J., Christensen, J. H., & Bouyssiere, B. (2023). Sustainable harnessing of SiO_2 nanoparticles from rice husks: A review of the best synthesis and applications. *Processes, 11*(12), 3373. https://doi.org/10.3390/pr11123373

Samarasekara, P., & Premasiri, N. G. K. V. M. (2016). Optical properties of spin coated and sol-gel dip coated cupric oxide thin films. *GESJ: Physics, 1*(15), 27–33. https://gesj.internet-academy.org.ge/en/list_artic_en.php?b_sec=phys&issue=2016-06

Sarma, M., Jaiswal, M. K., Podder, S., Bora, J., Karmakar, S., Choudhury, B., & Pal, A. R. (2023). A study on the applicability of thin film over powder for visible light photocatalysis. *Physica B: Condensed Matter, 670*, 415354. https://doi.org/10.1016/j.physb.2023.415354

Ulfa, M., Al Afif, H., Saraswati, T. E., & Bahruji, H. (2022). Fast removal of methylene blue via adsorption-photodegradation on TiO_2/SBA-15 synthesized by slow calcination. *Materials, 15*(16), 5471. https://doi.org/10.3390/ma15165471

Walker, J., & Koutsos, V. (2023). Spin coating of silica nanocolloids on mica: Self-assembly of two-dimensional colloid crystal structures and thin films. *Coatings, 13*(9), 1488. https://doi.org/10.3390/coatings13091488